

HiFi-Portrait: Zero-shot Identity-preserved Portrait Generation with High-fidelity Multi-face Fusion

Yifang Xu^{1*} Benxiang Zhai^{1*} Yunzhuo Sun² Ming Li³ Yang Li¹ Sidan Du^{1†}

¹Nanjing University ²Dalian University of Technology ³Nanjing University of Information Science and Technology
 {xyf, zbx}@smail.nju.edu.cn, sunyunzhuomail.dlut.edu.cn, mingli@nuist.edu.cn, {yogo, coff128}@nju.edu.cn

Abstract

Recent advancements in diffusion-based technologies have made significant strides, particularly in identity-preserved portrait generation (IPG). However, when using multiple reference images from the same ID, existing methods typically produce lower-fidelity portraits and struggle to customize face attributes precisely. To address these issues, this paper presents **HiFi-Portrait**, a **high-fidelity** method for zero-shot **portrait** generation. Specifically, we first introduce the face refiner and landmark generator to obtain fine-grained multi-face features and 3D-aware face landmarks. The landmarks include the reference ID and the target attributes. Then, we design HiFi-Net to fuse multi-face features and align them with landmarks, which improves ID fidelity and face control. In addition, we devise an automated pipeline to construct an ID-based dataset for training HiFi-Portrait. Extensive experimental results demonstrate that our method surpasses the SOTA approaches in face similarity and controllability. Furthermore, our method is also compatible with previous SDXL-based works.

1. Introduction

Identity-preserved portrait generation (IPG) has garnered significant attention in the past few years because of its potential applications in image animation, virtual try-ons, and e-commerce advertising. It aims to customize portraits consistent with the reference ID. Early approaches [11, 48], constrained by the capabilities of generative model [21], suffered from poor face similarity and image diversity. Thanks to the rapid advancement of large-scale text-image datasets [40, 46] and text-to-image diffusion models [42, 45], some methods fine-tune UNet [19, 43] or LoRA [26, 34, 44, 54] to create true-to-reality portraits. However, this fine-tuning typically requires at least 30 minutes per ID, which limits their practicality.

Recently, some studies [14, 23, 27, 51, 53, 55, 57, 59, 61, 64, 67] introduce a zero-shot setup, enabling portrait gener-

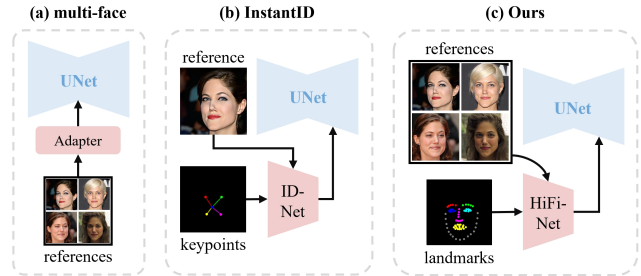


Figure 1. (a) Previous multi-face methods lack face location information, obtaining poor results. (b) InstantID only utilizes a single reference image, which limits its performance. (c) Our method fuses multi-faces and aligns them with landmarks via HiFi-Net, achieving high-fidelity ID-preservation. For a more concise presentation, we omit the face encoder.

ation within seconds without fine-tuning during inference. Among them, InstantID [51] is a representative work, as depicted in Fig. 1 (b), utilizing five keypoints (from target face) to guide the reference face in IdentityNet to achieve realistic IPG. Yet, it only considers one reference image during training, limiting its performance. Inspired by face feature fusion [28], some follow-up works [14, 32, 64] attempt using Adapter [61] to inject multi-face embeddings from the same ID, as illustrated in Fig. 1 (a). However, these methods tend to generate lower-fidelity portraits due to two factors: (1) Adapter provides weaker control compared to IdentityNet [51], and (2) the absence of facial positional guidance during multi-face fusion, resulting in inadequate multi-face alignment. In addition, all the above approaches cannot precisely control facial expressions and postures by relying solely on text prompts.

To address the aforementioned challenges, this paper proposes HiFi-Portrait for zero-shot IPG, a high-fidelity framework incorporating multi-face fusion, as illustrated in Fig. 2 and 3. To preserve more fine-grained ID information, we first design the face refiner to encode local and global facial features, generating multi-face features. Next, we introduce HiFi-Net to integrate these multi-face features and align them with 3D-aware face landmarks, thus enhancing

* Equal contributions. † Corresponding author.

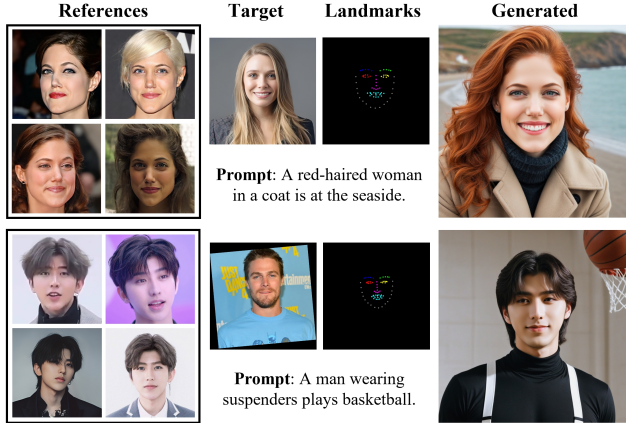


Figure 2. Given one or multiple reference images from the same person, **HiFi-Portrait** aims to generate high-fidelity portraits preserving the reference ID, where facial expressions and poses follow the target image, while other attributes (such as image background) are personalized via text prompt.

ID similarity. The landmarks consist of the reference face ID and the expression and pose customized by the target face. Besides, we devise a data collection pipeline to build a diverse ID-oriented dataset, where each ID contains multiple portraits with different attributes and captions. Using this type of data ensures that the model adheres to the guidance of landmarks and text prompts, avoiding direct replication of the reference face. In summary, our primary contributions include:

- We propose **HiFi-Portrait**, a tuning-free method for IPG with high-fidelity, which utilizes HiFi-Net to fuse multi-face features and align them with the landmarks.
- We collect a high-quality **ID-based dataset** consisting of 34k IDs and 960k text-portrait pairs, designed explicitly for training HiFi-Portrait.
- **High-fidelity.** Qualitative and quantitative experiments demonstrate that our method outperforms the SOTA approaches in face similarity and controllability.
- **Compatibility.** Our method is compatible with existing SDXL-based works, achieving high-quality multi-style generation.

2. Related Work

2.1. Text-to-Image Diffusion Models.

Diffusion models (DMs) [25, 36, 47] recently made significant advancements in image synthesis, which has attracted considerable attention. Compared to autoregressive models [30] and generative adversarial networks [21, 39], text-to-image DMs [22, 41, 45, 62] excel in generating diverse and high-quality images based on user-provided text prompts. A representative example is Stable Diffusion (SD) [42], which utilizes the CLIP [40] text encoder to obtain text embeddings

and then guide the denoising process through cross-attention mechanisms. Moreover, it performs denoising in latent space, thus significantly saving computational resources. Building on this, SDXL [38] enhances textual control by expanding the U-Net architecture and incorporating an additional text encoder.

2.2. ID-Preserved Portrait Generation.

The goal of IPG is to generate portraits that are consistent with the reference ID, while being personalized based on given conditions (e.g., textual prompt, depth map) [19, 43, 54, 56]. Initially, Textual Inversion [19] achieves this by training text embeddings with multiple images of the same ID. DreamBooth [43] accomplishes this through fine-tuning UNet. To reduce trainable parameters, some works train low-rank adaptation [26, 44, 54] to preserve facial ID. However, all the above methods require at least 30 minutes of individual training for each ID during inference, which is highly time-consuming and the applicability of IPG.

2.3. Zero-shot ID-Preserved Portrait Generation.

Some recent studies [14, 23, 27, 51, 53, 55, 58, 60, 61] introduce zero-shot IPG, which leverages large-scale text-image datasets to train models. During inference, these models customize portraits within seconds using reference images without additional fine-tuning. For instance, IP-Adapter-FaceID [14] trains Adapter (consisting of projection layer and cross-attention) to inject face embeddings and maintain ID consistency. However, the limited parameters in Adapter restrict the ID fidelity of results. To address this, the existing SOTA method, InstantID [51], utilizes five face keypoints to guide the face embeddings in IdentityNet. IdentityNet’s architecture is similar to that of ControlNet [63], but its inputs and conditions are the keypoints and face embeddings, respectively. However, InstantID only utilizes one reference face, which limits its performance.

To enhance facial similarity, subsequent zero-shot approaches [14, 32, 64] employ the “multi-face” strategy, which uses multiple reference images of the same individual for training. PhotoMaker [32] and IDAdapter [14] incorporate multi-face embeddings through cross-attention. FlashFace extends this approach by additionally training a face encoder to strengthen ID control. Nevertheless, these multi-face methods ignore the combination of local and global facial features. Moreover, they lack guidance regarding facial position information, leading to low fidelity of generated results. To tackle these challenges, this paper proposes HiFi-Portrait, which fuses multi-face features guided by the landmarks, thus enhancing ID fidelity. In addition, we collect an ID-driven dataset to train our model, thereby further improving ID similarity.

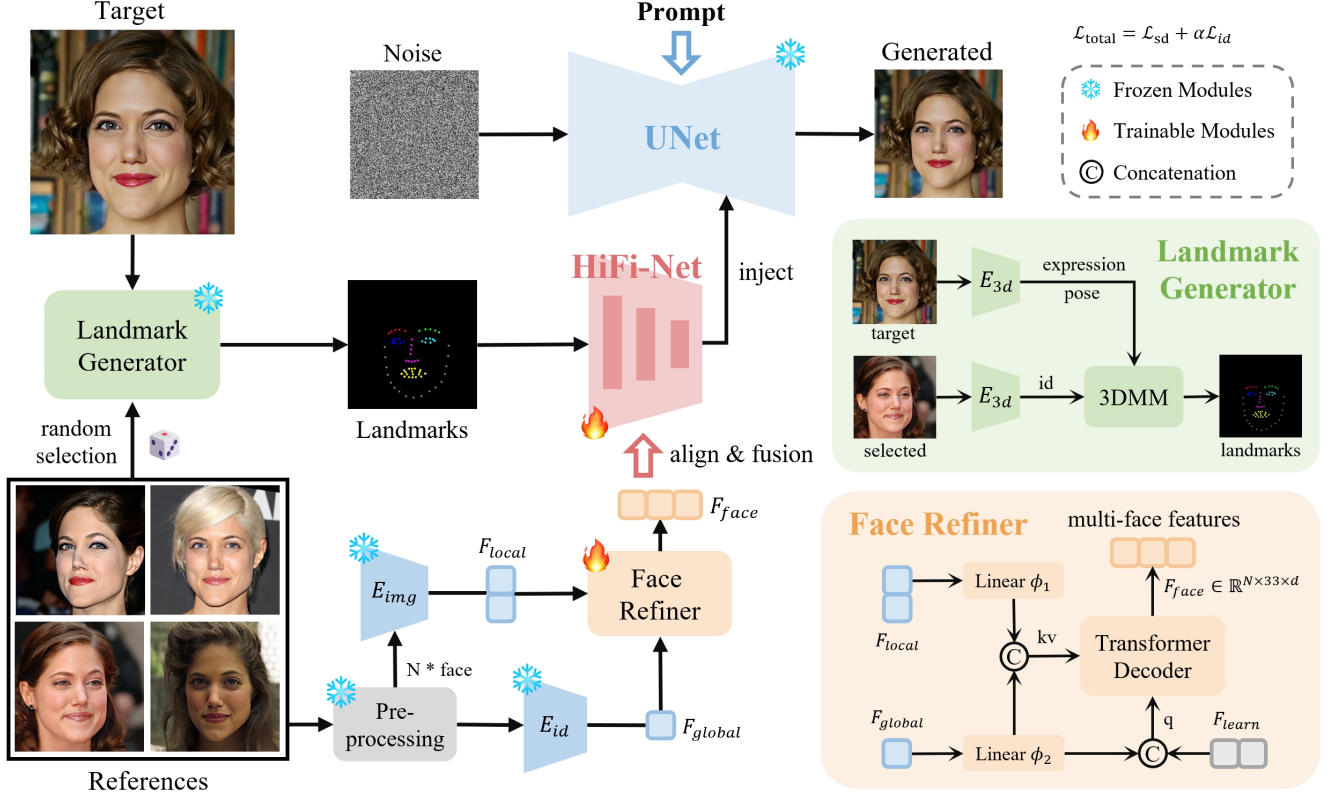


Figure 3. **The overall framework of HiFi-Portrait.** It consists of three key modules: (1) the face refiner merges local and global facial features to retain ID details. (2) the landmark generator produces 3D-aware landmarks, providing accurate guidance for facial control. (3) HiFi-Net fuses multi-face features and aligns them with landmarks, improving ID fidelity and controllability.

3. Method

In this section, we first review the principles of text-to-image diffusion models (Sec. 3.1). Next, Sec. 3.2 elaborates on the module and design motivation of HiFi-Portrait. Sec. 3.3 introduces the training and inference processes. Finally, Sec. 3.4 details the pipeline for constructing an ID-oriented dataset.

3.1. Preliminary

We build our method on SDXL [38], which enhances efficiency by projecting data into low-dimensional latent spaces. Specifically, SDXL first employs VAE [29] encoder \mathcal{E} to compress the given image $x_0 \in \mathbb{R}^{H \times W \times 3}$ into a latent code $z = \mathcal{E}(x_0) \in \mathbb{R}^{\frac{H}{8} \times \frac{W}{8} \times 4}$. Subsequently, the temporal-conditional UNet denoiser ϵ_θ estimates the noise added at the different timestep. The training objective can be defined as follows:

$$\mathcal{L} = \mathbb{E}_{z_t, t, c, \epsilon \sim \mathcal{N}(0,1)} [\|\epsilon - \epsilon_\theta(z_t, t, c)\|_2] \quad (1)$$

where z_t represents noisy latent at the t -th timestep. c denotes the text embeddings encoded by the CLIP text encoder. ϵ is ground-truth noise sampled from a standard Gaussian distribution.

3.2. HiFi-Portrait

Overview. Given N reference images $I_{ref} \in \mathbb{R}^{N \times H \times W \times 3}$ of the same individual, HiFi-Portrait aims to generate high-fidelity portrait $\hat{x}_0 \in \mathbb{R}^{H \times W \times 3}$ preserving the reference ID, where facial expressions and poses follow the target image $I_{tgt} \in \mathbb{R}^{H \times W \times 3}$, while other attributes (such as image style and background) are customized via text prompt.

Fig. 3 depicts the overall framework of HiFi-Portrait. It comprises three key components: (1) face refiner, which integrates local and global facial features to preserve detailed ID information. (2) landmark generator, creating 3D prior landmarks for accurate facial control. (3) HiFi-Net, which aligns and fuses multi-face features to enhance ID-fidelity.

Pre-processing. For the given reference images I_{ref} , we first apply PP-Matting [12] for human matting to remove the cluttered background in I_{ref} . Next, we employ the face detection model E_{det} [16] to obtain the highest-scoring faces $I_{face} \in \mathbb{R}^{N \times h \times w \times 3}$.

Face encoder. We then encode the reference faces I_{face} into facial features at different granularities. Specifically, we utilize the CLIP image encoder E_{img} to derive local facial features $F_{local} = E_{img}(I_{face}) \in \mathbb{R}^{N \times 257 \times d_1}$. Subse-

quently, we use the identity extractor E_{id} [15], pre-trained on face recognition and person re-identification, to obtain global facial features $F_{global} = E_{id}(I_{face}) \in \mathbb{R}^{N \times 1 \times d_2}$.

Face refiner. Since F_{local} contains fine-grained facial appearance, F_{global} contains key facial ID, they are complementary. A simple approach is concatenating and inputting them into HiFi-Net. However, prior research [51] indicates that using F_{local} can result in the direct pasting of blurred reference faces onto the generated images, thereby reducing face similarity. Thus, we design the face refiner to address this issue.

Specially, we first employ linear layers ϕ_1 and ϕ_2 for mapping F_{local} and F_{global} to the same dimension d , where $F'_{local} = \phi_2(F_{local}) \in \mathbb{R}^{N \times 257 \times d}$ and $F'_{global} = \phi_1(F_{global}) \in \mathbb{R}^{N \times 1 \times d}$. Then, we leverage the transformer decoder [49] with learnable face tokens $F_{learn} \in \mathbb{R}^{N \times 32 \times d}$ to extract ID details from F'_{local} and F'_{global} , thereby generating multi-face features $F_{face} \in \mathbb{R}^{N \times 33 \times d}$. Here, we concatenate F_{global} with F_{learn} as *query*, and concatenate F_{global} with F_{local} as *key* (*value*). The above process can be defined as follows:

$$q = \text{concat}(F'_{global}, F_{learn}) \quad (2)$$

$$kv = \text{concat}(F'_{global}, F'_{local}) \quad (3)$$

$$F_{face} = \text{Decoder}(q, kv) \quad (4)$$

Landmark generator. As shown in Fig. 3, we first utilize the 3D reconstruction network, DECA [18], to extract facial ID, expression, and pose vectors from reference and target images. Subsequently, we combine the reference ID with target expression and pose vectors, then render a new 3D face using the 3D Morphable Model (3DMM) fitting algorithm [9]. Finally, we project the 3D face onto the 2D plane, resulting in 3D-aware face landmarks $I_{lmk} \in \mathbb{R}^{H \times W \times 3}$.

HiFi-Net. To enhance ID fidelity, we input conditions I_{lmk} and F_{face} into HiFi-Net, a network architecture derived from ControlNet [63]. Specifically, the VAE first embeds I_{lmk} into latent space, yielding latent code $z_{lmk} \in \mathbb{R}^{\frac{H}{8} \times \frac{W}{8} \times 4}$. Subsequently, z_{lmk} guides the fusion and alignment of F_{face} into the latent spaces, facilitated by the cross-attention mechanism within HiFi-Net. This process is mathematically represented as follows:

$$\text{Attention}(Q, K, V) = \text{softmax} \left(\frac{QK^T}{\sqrt{d_k}} \right) V \quad (5)$$

where $Q = \phi_q(z_{lmk})$, $K = \phi_k(F'_{face})$, and $V = \phi_v(F'_{face})$ represent the *query*, *key*, and *value* respectively. $F'_{face} \in \mathbb{R}^{(N \times 33) \times d}$ denotes the flattened F_{face} . The functions ϕ_q , ϕ_k , and ϕ_v are linear layers. Finally, HiFi-Net yields high-fidelity identity features c_{id} , which are injected into the UNet denoiser to preserve facial identity effectively. The architecture of HiFi-Net can be found in the **Appendix**.

3.3. Model Training and Inference

Training. During training, we randomly select one image from I_{ref} , and feed it into the landmark generator to obtain the reference ID. We only train the parameters of the face refiner and HiFi-Net, while the other modules remain frozen. The optimization objective of SD is as follows:

$$\mathcal{L}_{sd} = \|\epsilon - \epsilon_\theta(z_t, t, c, c_{id})\|_2 \quad (6)$$

In addition, we follow previous works [14, 15], employing the face ID loss \mathcal{L}_{id} to improving ID fidelity.

$$\mathcal{L}_{id} = E_{det}(\hat{x}_0) \cdot [1 - \cos(F_{id}, E_{id}(\hat{x}_0))] \quad (7)$$

Here, \cos is the cosine similarity. $F_{id} = \text{avg}[E_{id}(I_{face})] \in \mathbb{R}^{1 \times d_2}$ represents the average reference ID features. \hat{x}_0 denotes the generated denoised image. We use E_{det} to prevent the unclear face in \hat{x}_0 from misleading the model. When a face is detected in \hat{x}_0 , $E_{det}(\hat{x}_0) = 1$; otherwise $E_{det}(\hat{x}_0) = 0$. Finally, the total loss with $\alpha = 0.1$ is as follows:

$$\mathcal{L}_{total} = \mathcal{L}_{sd} + \alpha \mathcal{L}_{id} \quad (8)$$

Inference. During inference, we compute the face score $S_{ref} \in \mathbb{R}^N$ for the given N reference images I_{ref} (see Eq. 9). Subsequently, we select the highest-scoring reference image into the landmark generator to get reference

$$S_{ref} = S_q(I_{ref}) + \lambda S_a(I_{ref}, I_{tgt}) \quad (9)$$

where S_q represents the face quality score estimated by ModelScopeFQA [35]. S_q is higher for images with greater facial clarity and minimal obstructions. S_a is the face angle score calculated by RetinaFace [16]. Using S_a aims to select the images that are more consistent with the angle of target image I_{tgt} , which reduces the loss of ID information in 3DMM. λ is set to 0.5, balancing the influence of quality and angle in the face score.

3.4. ID-based Dataset Construction Pipeline

To enhance ID fidelity, HiFi-Portrait requires multiple images from the same ID for training. However, existing datasets in multi-face IPG methods [32, 64] are not yet open-source. To address this, we devise a high-quality pipeline for creating an ID-based dataset. This dataset includes an average of 28 text-image pairs per ID, with images featuring diverse expressions, poses, hairstyles, and other attributes. We believe that this dataset will advance future ID-based (multi-face) research.

Data collection. We utilize the open-source datasets VGGFace2-HD [10, 13] and IMDb-Face [50] for our research. For IMDb-Face, we download raw images from all valid source urls. To enhance ID diversity, we additionally gather a list of celebrities from not included in IMDb-Face. Based on this list, we collect approximately 100 images per name via search engines.

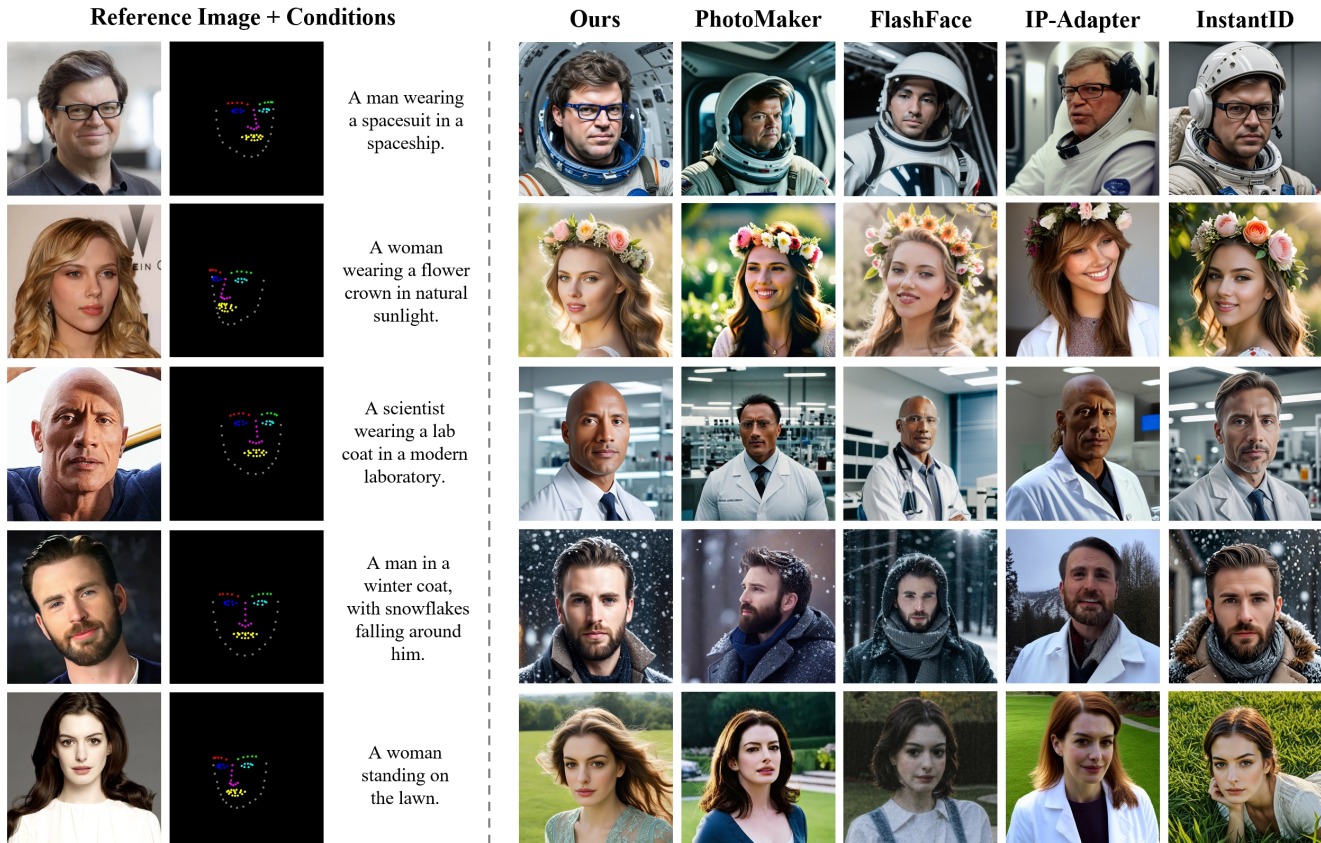


Figure 4. **Qualitative results.** We compare HiFi-Portrait with four of the SOTA open-source techniques: PhotoMaker [32], FlashFace [64], IP-Adapter [61], and InstantID [51]. All methods use 4 reference portraits from the same ID. We observe that our framework achieves high-fidelity portrait generation with ID preservation, with precise control over image attributes facilitated by conditions (landmarks and text prompts).

Face detection. We initially apply RetinaFace to detect face and obtain bounding boxes, deleting images where the number of faces is not equal to 1. Subsequently, we crop images to larger squares according to the bounding boxes, ensuring the face occupies more than 10% of the cropped area. In addition, images smaller than 256×256 are discarded, and all remaining images are resized to 1024×1024 .

Data cleansing. To improve the dataset quality, we perform the following steps to eliminate noisy images. First, we employ ModelScopeFQA to assess face quality scores, removing images with scores below 0.45. Next, we use PaddleOCR [4] to recognize and delete images with watermarks on faces. To minimize images with occluded faces, we leverage BLIP-2 [31] to generate facial descriptions, filtering out images that contain foreign objects (e.g., hand, microphone) in the descriptions. Finally, GFPGAN [52] is used for face restoration.

Face verification. To identify images belonging to the current ID group, we extract face embeddings via InsightFace [15]. Then, we adopt k-means clustering algorithm to choose

the central embedding of the largest cluster as the target embedding. Finally, we only save images that similarity with target embedding higher than 0.7, effectively removing images from other IDs.

Image caption. Although the landmarks encompass the individual’s expressions and poses, to ensure the diversity of the generated images, we prompt Yi-Vision [8] for detailed image captions using the following prompt: *”Dear Yi-Vision, please describe this portrait in detail, focusing on the person’s appearance, hairstyle, clothing, accessories, and background. Please do not describe facial expressions and poses.”*

Data statistics. Finally, using the proposed pipeline, we create a training dataset comprising 34k IDs and 960k images, with an average of 28 images per ID. For more detailed dataset statistics, please read the *appendix*.

4. Experiments

4.1. Experimental Settings

Implementation details. Our framework is based on SDXL-base-1.0 [6, 38] with the dimension $d = 2048$.

Table 1. **Quantitative comparison** of HiFi-Portrait and state-of-the-art methods. All metrics are in percentages (%). The best results are highlighted in **bold**.

Method	WebFace-100					InternetFace-300				
	$Sim_f \uparrow$	$CLIP_f \uparrow$	$Exp \downarrow$	$Pose \downarrow$	$FID \downarrow$	$Sim_f \uparrow$	$CLIP_f \uparrow$	$Exp \downarrow$	$Pose \downarrow$	$FID \downarrow$
PhotoMaker [32]	46.6	48.0	23.1	8.3	121.8	37.1	44.3	24.7	9.5	189.8
ConsistentID [27]	61.4	58.5	22.7	8.0	118.3	54.2	56.1	24.3	8.7	182.4
FlashFace [64]	64.3	70.2	20.9	7.9	123.4	60.4	71.4	22.5	8.3	173.5
IP-Adapter [61]	64.1	65.6	20.3	8.5	120.7	62.3	63.2	23.1	8.2	176.2
InstantID [51]	72.9	68.2	18.8	6.1	114.4	69.7	67.8	20.4	6.7	158.1
HiFi-Portrait (Ours)	77.7	72.4	14.7	5.4	108.5	73.1	71.1	16.9	6.2	163.4



Figure 5. **Compatibility**. Our method is compatible with models of different styles, which can generate diverse and high-quality images with high-fidelity ID preservation.

$d_1 = 1280$, $d_2 = 512$. Correspondingly, the training images are resized to 1024×1024 . The number of transformer decoder layers in the face refiner is set to 5. For the CLIP encoder, we utilize clip-vit-large-patch14 [40] pretrained by OpenAI. During training, we randomly select 1 image from the same ID group as the target and N images as references, where N is randomly set between 1 and 4. An empty text prompt is also used with 10% probability to enhance generative performance through classifier-free guidance. We employ the Adam optimizer with a constant learning rate of $2e-5$. The model is trained using 4 NVIDIA A800 GPUs over 800k iterations (16 days), with a batch size 24. During inference, we set $N = 4$. Use DDIM [47] sampler with 8-steps SDXL-Lightning [33].

Evaluation datasets. To obtain quantitative results, we construct two evaluation datasets. Specifically, we randomly select 100 identities from the WebFace260M [66] dataset, referred to as WebFace-100. We collect 300 ID groups from the Internet that are not used in training, termed InternetFace-300. By leveraging the data processing described in Sec. 3.4, each ID group comprises 1 target image and 4 reference

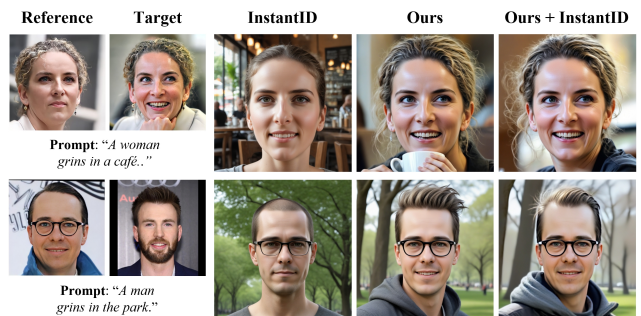


Figure 6. **HiFi-Portrait + InstantID**. The reference and target image in the top case are from the same ID. The bottom case from the different IDs.

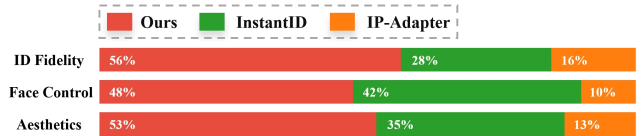


Figure 7. **User study**. Participants consistently prefer HiFi-Portrait in three aspects: ID fidelity, face controllability, and aesthetics.

images. The target image is randomly selected from LAION-Face [65]. We collect 10 diverse text prompts and generate 3 distinct images for each combination (prompt, ID group). In total, we generate 3,000 images for WebFace-100 and 9,000 images for InternetFace-300.

Evaluation metrics. We employ Sim_f and $CLIP_f$ to assess ID fidelity, where Sim_f ($CLIP_f$) represents the average cosine similarity of face (CLIP) embeddings between all reference faces and the generated face. These embeddings are extracted using InsightFace [15] (CLIP [40] image encoder). To evaluate face controllability, we use Exp and $Pose$, computed as the root mean squared error (RMSE) between the target and generated expression (pose) vectors, estimated by DECA [18]. Additionally, we utilize FID [24] to measure the generation quality.

4.2. Comparisons

Qualitative results. As illustrated in Fig. 4, we compare qualitatively with current SOTA methods [32, 51, 61, 64].



Figure 8. **Impact of face refiner.** Compared with "concat" (directly concatenate local and global features), using the face refiner to obtain multi-face features effectively captures the ID details from local and global features, thereby enhancing ID fidelity.

Table 2. Ablation on face refiner.

Method	$Sim_f \uparrow$	$CLIP_f \uparrow$
local features	62.3	55.2
global features	63.9	56.8
concat	64.4	57.3
face refiner	65.2	58.9

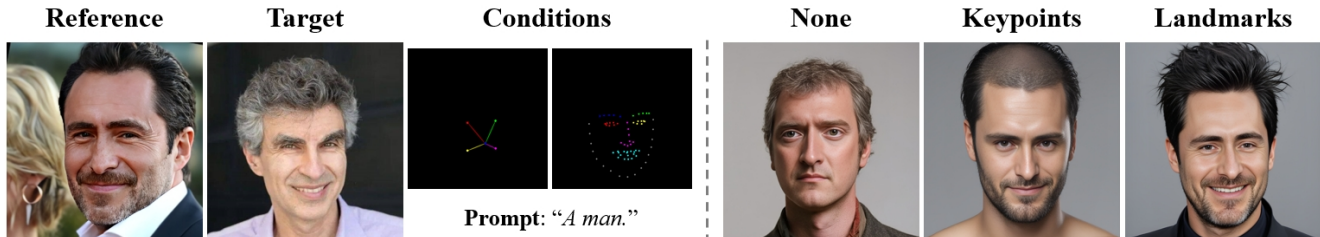


Figure 9. **Effect of HiFi-Net.** "None" utilizes Adapter that injects multi-face features through trainable cross-attention layers. "Keypoints" maintain HiFi-Net architecture but use face keypoints as input conditions. "Landmarks" represent using HiFi-Net. Using landmarks to guide the fusion of multi-face features and aligning them in HiFi-Net achieves high-fidelity results.

For a fair comparison, we employ the optimal versions of IP-Adapter [3] and InstantID [20]. All methods use 4 reference portraits from the same ID. To facilitate comparison, we only show 1 reference portrait. The results show that our method leverages face landmarks, which offer customizable facial expressions and poses, unlike previous multi-face methods [32, 64] without face location information. Compared to all evaluated methods, HiFi-Portrait achieves superior ID preservation, enhanced facial controllability, and better aesthetics.

Quantitative results. Tab. 1 presents the qualitative comparisons on evaluation datasets. To ensure fairness, we inject landmark images via ControlNet [63] for all methods [27, 32, 61, 64] that lack control information. The results demonstrate that our proposed HiFi-Portrait outperforms existing methods in ID fidelity (Sim_f , $CLIP_f$). This is attributed to the utilization of the face refiner and HiFi-Net, which facilitate the generation of high-fidelity face features. Moreover, our approach achieves superior results in Exp and $Pose$, benefiting from the guided fusion of multi-face features by face landmarks in HiFi-Net for precise facial control. Furthermore, our method generates high-quality images with clear advantages in FID scores.

User study. To further demonstrate the superiority of HiFi-Portrait, we randomly select 20 IDs (5 prompts, 3 seeds) from WebFace-100 and generate results using each method. Twenty users rate the images based on ID fidelity, face controllability, and aesthetic quality. As shown in Fig. 7, our model consistently receives the highest preference across all

Table 3. Ablation on HiFi-Net.

HiFi-Net	Condition	$Sim_f \uparrow$	$CLIP_f \uparrow$	$Exp \downarrow$	$Pose \downarrow$
✗	✗	61.8	52.5	22.7	8.4
✓	keypoints	64.5	58.1	19.8	7.2
✓	landmarks	65.2	58.9	18.4	6.8

metrics.

Compatibility. In Fig. 5, we utilize SDXL-based models (including 3D cartoon [1], 2D anime [7] and pixel art [5]) to generate images with different styles. As can be seen from the displayed results, although HiFi-Portrait focuses on real-life portrait generation, it can still be used to generate images of different styles and achieve high-fidelity ID preservation. This also illustrates the diversity and compatibility of our approach.

Fig. 6 demonstrates the results when HiFi-Portrait is combined with InstantID. The comparison reveals that InstantID, relying solely on text prompts and face keypoints, fails to control facial expressions precisely. In contrast, our method leverages face landmarks to accurately dictate expressions and poses accurately, achieving superior ID fidelity. Moreover, HiFi-Portrait is also compatible with InstantID.

4.3. Ablation Studies

Following previous works [32, 64], we shortened the total number of training steps to one-eighth to allow for ablations on each trainable module. All ablations are performed on WebFace-100.

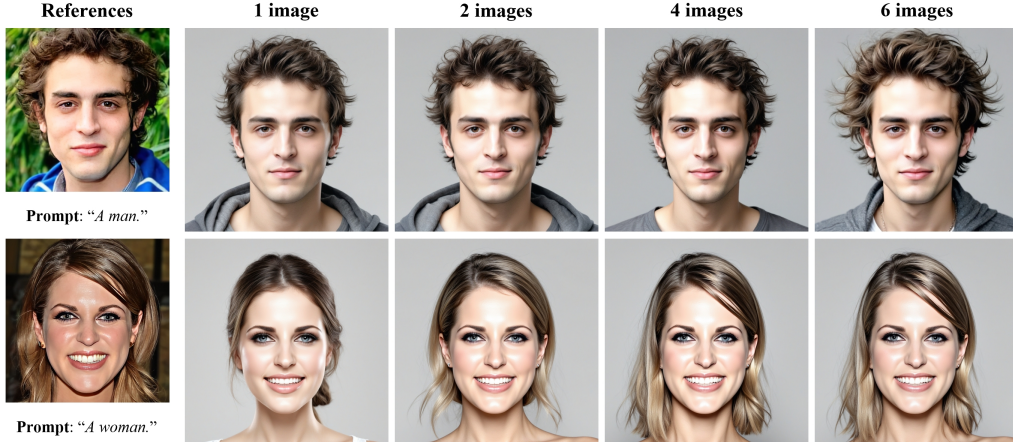


Table 4. Ablation on the number of reference images.

N	$Sim_f \uparrow$	$CLIP_f \uparrow$
1	61.9	52.3
2	63.8	56.7
3	64.6	57.1
4	65.2	58.9
5	65.0	58.6
6	64.8	58.5

Figure 10. **Impact of the number of reference images.** The reference and target images originating from the same ID. The results indicate that ID fidelity improves with an increasing number of reference images, underscoring the effectiveness of our multi-face fusion strategy.

Impact of face refiner. Tab. 2 illustrates the influence of face refiner on maintaining ID similarity. Rows 1 to 3 correspond to local features, global features, and their concatenation are respectively fed into the HiFi-Net. Note that they are all multi-face features. Fig. 8 presents the visual results that utilize various facial features. Experimental results show that both local and global features contribute to preserving ID. Utilizing the face refiner enhances ID details in multi-face features, auguring ID fidelity.

Impact of HiFi-Net. In Tab. 3, we investigate the impact of HiFi-Net. Row 1 represents HiFi-Net and facial location information is not utilized, instead employing Adapter (trainable cross-attention layers) [61] to inject multi-face features into the UNet. Rows 2 and 3, building on HiFi-Net, leverage face keypoints and landmarks as conditional inputs, respectively. In addition, we visualize generated results under different conditions, as shown in Fig. 9. Results indicate that Adapter yields poor outcomes due to the lack of guidance on facial location. Utilizing keypoints within HiFi-Net produces moderate results but lacks control over facial expressions. Conversely, using landmarks to guide multi-face feature fusion within HiFi-Net enhances face fidelity and controllability.

The number of reference images N . Tab. 4 reports on the effect of using different numbers of reference images during inference. Compared with $N = 1$, notable improvements are observed when $N = 2$. The best results are achieved when $N = 4$. In the Fig. 10, we visualize the effect of the number of reference images on the generated results. It can be seen that the ID fidelity increases as the number of reference images increases

Effect of landmark selection. Tab. 5 explores the effect of the selected image in landmark generator during inference. Row 1 directly uses target landmarks (ID, pose, expression

Table 5. Ablation on landmark selection.

Method	$Sim_f \uparrow$	$CLIP_f \uparrow$	$Exp \downarrow$	$Pose \downarrow$
target	60.2	56.4	18.0	6.6
random	64.5	58.2	18.8	7.1
quality	64.8	58.7	18.2	6.9
angle	64.9	58.4	18.5	6.8
manual	65.1	58.7	18.6	6.9
quality & angle	65.2	58.9	18.2	6.8

from target), resulting in lower ID fidelity. Compared to randomly selecting a reference image (row 2), choosing images with the highest face quality score or angle score (row 6) yields better performances. Row 5 is derived by manually selecting high-quality images with face angles close to the target image. In practical applications, allowing user manual selection might be considered. Compared to cumbersome manual selection, row 6 employs face quality and angle scores, improving ID fidelity while maintaining robust facial control. Therefore, row 6 is adopted during inference.

5. Conclusion

This paper presents HiFi-Portrait, a high-fidelity ID-preserved framework for zero-shot portrait generation. To achieve this, we design the face refiner and landmark generator to obtain multi-face features and 3D-aware face priors. Next, we develop HiFi-Net leveraging landmark conditioning to effectively guide the fusion of multi-face features, which enhances ID fidelity and face controllability. Finally, we engineer an automated pipeline to collect an ID-based dataset, facilitating the training of HiFi-Portrait. Compared with the SOTA methods, our approach can generate more high-quality portraits with customizable facial attributes, while maintaining strong ID fidelity. More discussions can be found in *appendix*.

References

- [1] 3D rendering style - 3DMM_XL_V13 | Stable Diffusion XL LoRA | Civitai, 2023. 7
- [2] Black-forest-labs/FLUX.1-dev · Hugging Face, 2024. 5
- [3] H94/IP-Adapter-FaceID · Hugging Face, 2024. 7
- [4] PaddlePaddle/PaddleOCR. PaddlePaddle, 2024. 5
- [5] Pixel Art Diffusion XL - Sprite Shaper | Stable Diffusion XL Checkpoint | Civitai, 2024. 7
- [6] Stabilityai/stable-diffusion-xl-base-1.0 · Hugging Face, 2024. 5
- [7] SDXL Yamer's Anime Unstable Illustrator - Stage Anima | Stable Diffusion XL Checkpoint | Civitai, 2024. 7
- [8] 01 AI, Alex Young, Bei Chen, Chao Li, Chengen Huang, Ge Zhang, and Guanwei Zhang. Yi: Open Foundation Models by 01.AI, 2024. 5
- [9] Volker Blanz and Thomas Vetter. A morphable model for the synthesis of 3D faces. In *SIGGRAPH*, pages 187–194, Not Known, 1999. ACM Press. 4
- [10] Qiong Cao, Li Shen, Weidi Xie, Omkar M. Parkhi, and Andrew Zisserman. Vggface2: A dataset for recognising faces across pose and age. In *2018 13th IEEE International Conference on Automatic Face & Gesture Recognition (FG 2018)*, pages 67–74. IEEE, 2018. 4, 1
- [11] Anpei Chen, Ruiyang Liu, Ling Xie, Zhang Chen, Hao Su, and Jingyi Yu. SofGAN: A Portrait Image Generator with Dynamic Styling. *ACM Transactions on Graphics*, 41(1): 1–26, 2022. 1
- [12] Guowei Chen, Yi Liu, Jian Wang, Juncai Peng, Yuying Hao, Lutao Chu, Shiyu Tang, Zewu Wu, Zeyu Chen, Zhiliang Yu, et al. Pp-matting: high-accuracy natural image matting. *arXiv preprint arXiv:2204.09433*, 2022. 3
- [13] Xuanhong Chen, Bingbing Ni, Yutian Liu, Naiyuan Liu, Zhilin Zeng, and Hang Wang. Simswap++: Towards faster and high-quality identity swapping. *IEEE TPAMI*, 2023. 4, 1
- [14] Siying Cui, Jia Guo, Xiang An, Jiankang Deng, Yongle Zhao, Xinyu Wei, and Ziyong Feng. IDAdapter: Learning Mixed Features for Tuning-Free Personalization of Text-to-Image Models, 2024. 1, 2, 4
- [15] Jiankang Deng, Jia Guo, Niannan Xue, and Stefanos Zafeiriou. Arcface: Additive angular margin loss for deep face recognition. In *CVPR*, pages 4690–4699, 2019. 4, 5, 6, 2
- [16] Jiankang Deng, Jia Guo, Evangelos Ververas, Irene Kotsia, and Stefanos Zafeiriou. Retinaface: Single-shot multi-level face localisation in the wild. In *CVPR*, pages 5203–5212, 2020. 3, 4, 2
- [17] Patrick Esser, Sumith Kulal, Andreas Blattmann, Rahim Entezari, Jonas Müller, Harry Saini, Yam Levi, Dominik Lorenz, Axel Sauer, and Frederic Boesel. Scaling rectified flow transformers for high-resolution image synthesis. In *ICML*, 2024. 5
- [18] Yao Feng, Haiwen Feng, Michael J. Black, and Timo Bolkart. Learning an animatable detailed 3D face model from in-the-wild images. *ACM Transactions on Graphics (ToG)*, 40(4): 1–13, 2021. 4, 6
- [19] Rinon Gal, Yuval Alaluf, Yuval Atzmon, Or Patashnik, Amit H. Bermano, Gal Chechik, and Daniel Cohen-Or. An image is worth one word: Personalizing text-to-image generation using textual inversion. *arXiv preprint arXiv:2208.01618*, 2022. 1, 2
- [20] GitHub. Instantid-full, 2024. 7
- [21] Ian Goodfellow, Jean Pouget-Abadie, Mehdi Mirza, Bing Xu, David Warde-Farley, Sherjil Ozair, Aaron Courville, and Yoshua Bengio. Generative adversarial nets. *NeurIPS*, 27, 2014. 1, 2
- [22] Shuyang Gu, Dong Chen, Jianmin Bao, Fang Wen, Bo Zhang, Dongdong Chen, Lu Yuan, and Baining Guo. Vector quantized diffusion model for text-to-image synthesis. *arXiv preprint arXiv:2111.14822*, 2021. 2
- [23] Zinan Guo, Yanze Wu, Zhuowei Chen, Lang Chen, and Qian He. PuLID: Pure and Lightning ID Customization via Contrastive Alignment, 2024. 1, 2
- [24] Martin Heusel, Hubert Ramsauer, Thomas Unterthiner, Bernhard Nessler, and Sepp Hochreiter. Gans trained by a two time-scale update rule converge to a local nash equilibrium. *Advances in neural information processing systems*, 30, 2017. 6
- [25] Jonathan Ho, Ajay Jain, and Pieter Abbeel. Denoising diffusion probabilistic models. *NeurIPS*, 33:6840–6851, 2020. 2
- [26] Edward J. Hu, Yelong Shen, Phillip Wallis, Zeyuan Allen-Zhu, Yuanzhi Li, Shean Wang, Lu Wang, and Weizhu Chen. Lora: Low-rank adaptation of large language models. *arXiv preprint arXiv:2106.09685*, 2021. 1, 2
- [27] Jiehui Huang, Xiao Dong, Wenhui Song, Hanhui Li, Jun Zhou, Yuhao Cheng, Shutao Liao, Long Chen, Yiqiang Yan, Shengcai Liao, and Xiaodan Liang. ConsistentID: Portrait Generation with Multimodal Fine-Grained Identity Preserving, 2024. 1, 2, 6, 7
- [28] Bhavin Jawade, Deen Dayal Mohan, Dennis Fedorishin, Srirangaraj Setlur, and Venu Govindaraju. Conan: Conditional neural aggregation network for unconstrained face feature fusion. In *2023 IEEE International Joint Conference on Biometrics (IJCB)*, pages 1–10. IEEE, 2023. 1
- [29] Diederik P. Kingma and Max Welling. Auto-encoding variational bayes. *arXiv preprint arXiv:1312.6114*, 2013. 3
- [30] Hugo Larochelle and Iain Murray. The neural autoregressive distribution estimator. In *Proceedings of the Fourteenth International Conference on Artificial Intelligence and Statistics*, pages 29–37. JMLR Workshop and Conference Proceedings, 2011. 2
- [31] Junnan Li, Dongxu Li, Silvio Savarese, and Steven Hoi. Blip-2: Bootstrapping language-image pre-training with frozen image encoders and large language models. *arXiv preprint arXiv:2301.12597*, 2023. 5
- [32] Zhen Li, Mingdeng Cao, Xintao Wang, Zhongang Qi, Ming-Ming Cheng, and Ying Shan. PhotoMaker: Customizing Realistic Human Photos via Stacked ID Embedding, 2023. 1, 2, 4, 5, 6, 7
- [33] Shanchuan Lin, Anran Wang, and Xiao Yang. SDXL-Lighting: Progressive Adversarial Diffusion Distillation, 2024. 6, 5
- [34] Yang Liu, Cheng Yu, Lei Shang, Ziheng Wu, Xingjun Wang, Yuze Zhao, Lin Zhu, Chen Cheng, Weitao Chen, Chao Xu,

- Haoyu Xie, Yuan Yao, Wenmeng Zhou, Yingda Chen, Xun-song Xie, and Baigui Sun. FaceChain: A Playground for Identity-Preserving Portrait Generation, 2023. 1, 2
- [35] ModelScope. Computer vision, manual face quality assessment, 2020. 4
- [36] Alexander Quinn Nichol and Prafulla Dhariwal. Improved denoising diffusion probabilistic models. In *ICML*, pages 8162–8171. PMLR, 2021. 2
- [37] Bohao Peng, Jian Wang, Yuechen Zhang, Wenbo Li, Ming-Chang Yang, and Jiaya Jia. ControlNeXt: Powerful and Efficient Control for Image and Video Generation, 2024. 5
- [38] Dustin Podell, Zion English, Kyle Lacey, Andreas Blattmann, Tim Dockhorn, Jonas Müller, Joe Penna, and Robin Rombach. SDXL: Improving Latent Diffusion Models for High-Resolution Image Synthesis. *arXiv preprint arXiv:2307.01952*, 2023. 2, 3, 5
- [39] Alec Radford, Luke Metz, and Soumith Chintala. Unsupervised representation learning with deep convolutional generative adversarial networks. *arXiv preprint arXiv:1511.06434*, 2015. 2
- [40] Alec Radford, Jong Wook Kim, Chris Hallacy, Aditya Ramesh, Gabriel Goh, Sandhini Agarwal, Girish Sastry, Amanda Askell, Pamela Mishkin, and Jack Clark. Learning transferable visual models from natural language supervision. In *ICML*, pages 8748–8763. PMLR, 2021. 1, 2, 6
- [41] Aditya Ramesh, Prafulla Dhariwal, Alex Nichol, Casey Chu, and Mark Chen. Hierarchical text-conditional image generation with clip latents. *arXiv preprint arXiv:2204.06125*, 2022. 2
- [42] Robin Rombach, Andreas Blattmann, Dominik Lorenz, Patrick Esser, and Björn Ommer. High-Resolution Image Synthesis with Latent Diffusion Models. *arXiv preprint arXiv:2112.10752*, 2021. 1, 2
- [43] Nataniel Ruiz, Yuanzhen Li, Varun Jampani, Yael Pritch, Michael Rubinstein, and Kfir Aberman. Dreambooth: Fine tuning text-to-image diffusion models for subject-driven generation. In *CVPR*, pages 22500–22510, 2023. 1, 2
- [44] Nataniel Ruiz, Yuanzhen Li, Varun Jampani, Wei Wei, Tingbo Hou, Yael Pritch, Neal Wadhwa, Michael Rubinstein, and Kfir Aberman. HyperDreamBooth: HyperNetworks for Fast Personalization of Text-to-Image Models. *arXiv preprint arXiv:2307.06949*, 2023. 1, 2
- [45] Chitwan Saharia, William Chan, Saurabh Saxena, Lala Li, Jay Whang, Emily L. Denton, Kamyar Ghasemipour, Raphael Gontijo Lopes, Burcu Karagol Ayan, and Tim Salimans. Photorealistic text-to-image diffusion models with deep language understanding. *NeurIPS*, 35:36479–36494, 2022. 1, 2
- [46] Christoph Schuhmann, Romain Beaumont, Richard Vencu, Cade Gordon, Ross Wightman, Mehdi Cherti, Theo Coombes, Aarush Katta, Clayton Mullis, and Mitchell Wortsman. Laion-5b: An open large-scale dataset for training next generation image-text models. *NeurIPS*, 35:25278–25294, 2022. 1
- [47] Jiaming Song, Chenlin Meng, and Stefano Ermon. Denoising diffusion implicit models. *arXiv preprint arXiv:2010.02502*, 2020. 2, 6
- [48] Wanchao Su, Hui Ye, Shu-Yu Chen, Lin Gao, and Hongbo Fu. Drawinginstyles: Portrait image generation and editing with spatially conditioned stylegan. *IEEE transactions on visualization and computer graphics*, 29(10):4074–4088, 2022. 1
- [49] Ashish Vaswani, Noam Shazeer, Niki Parmar, Jakob Uszkoreit, Llion Jones, Aidan N. Gomez, \Lukasz Kaiser, and Illia Polosukhin. Attention is all you need. In *NeurIPS*, pages 5998–6008, 2017. 4
- [50] Fei Wang, Liren Chen, Cheng Li, Shiyao Huang, Yanjie Chen, Chen Qian, and Chen Change Loy. The devil of face recognition is in the noise. In *ECCV*, pages 765–780, 2018. 4, 1
- [51] Qixun Wang, Xu Bai, Haofan Wang, Zekui Qin, and Anthony Chen. InstantID: Zero-shot Identity-Preserving Generation in Seconds, 2024. 1, 2, 4, 5, 6
- [52] Xintao Wang, Yu Li, Honglun Zhang, and Ying Shan. Towards real-world blind face restoration with generative facial prior. In *CVPR*, pages 9168–9178, 2021. 5
- [53] Zhichao Wei, Qingkun Su, Long Qin, and Weizhi Wang. MM-Diff: High-Fidelity Image Personalization via Multi-Modal Condition Integration, 2024. 1, 2
- [54] Ziheng Wu, Jiaqi Xu, Xinyi Zou, Kunzhe Huang, Xing Shi, and Jun Huang. EasyPhoto: Your Smart AI Photo Generator, 2023. 1, 2
- [55] Peng Xing, Ning Wang, Jianbo Ouyang, and Zechao Li. Inv-Adapter: ID Customization Generation via Image Inversion and Lightweight Adapter, 2024. 1, 2
- [56] Yifang Xu, Chenglei Peng, Ming Li, Yang Li, and Sidan Du. Pyramid Feature Attention Network for Monocular Depth Prediction. In *ICME*, pages 1–6, 2021. 2
- [57] Yifang Xu, Yunzhuo Sun, Zien Xie, Benxiang Zhai, and Sidan Du. VTG-GPT: Tuning-Free Zero-Shot Video Temporal Grounding with GPT. *Applied Sciences-Basel*, 14(5):1894, 2024. 1
- [58] Yifang Xu, Yunzhuo Sun, Benxiang Zhai, Youyao Jia, and Sidan Du. MH-DETR: Video Moment and Highlight Detection with Cross-modal Transformer. In *IJCNN*, pages 1–8. IEEE, 2024. 2
- [59] Yifang Xu, Yunzhuo Sun, Benxiang Zhai, Zien Xie, Youyao Jia, and Sidan Du. Multi-Modal Fusion and Query Refinement Network for Video Moment Retrieval and Highlight Detection. In *ICME*, pages 1–6. IEEE, 2024. 1
- [60] Yifang Xu, Yunzhuo Sun, Benxiang Zhai, Ming Li, Wenxin Liang, Yang Li, and Sidan Du. Zero-shot video moment retrieval via off-the-shelf multimodal large language models. *arXiv preprint arXiv:2501.07972*, 2025. 2
- [61] Hu Ye, Jun Zhang, Sibao Liu, Xiao Han, and Wei Yang. IP-Adapter: Text Compatible Image Prompt Adapter for Text-to-Image Diffusion Models, 2023. 1, 2, 5, 6, 7, 8
- [62] Jiahui Yu, Yuanzhong Xu, Jing Yu Koh, Thang Luong, Gunjan Baid, Zirui Wang, Vijay Vasudevan, Alexander Ku, Yinfei Yang, and Burcu Karagol Ayan. Scaling autoregressive models for content-rich text-to-image generation. *arXiv preprint arXiv:2206.10789*, 2(3):5, 2022. 2
- [63] Lvmin Zhang and Maneesh Agrawala. Adding conditional control to text-to-image diffusion models. *arXiv preprint arXiv:2302.05543*, 2023. 2, 4, 7

- [64] Shilong Zhang, Lianghua Huang, Xi Chen, Yifei Zhang, Zhi-Fan Wu, Yutong Feng, Wei Wang, Yujun Shen, Yu Liu, and Ping Luo. FlashFace: Human Image Personalization with High-fidelity Identity Preservation, 2024. [1](#), [2](#), [4](#), [5](#), [6](#), [7](#)
- [65] Yinglin Zheng, Hao Yang, Ting Zhang, Jianmin Bao, Dongdong Chen, Yangyu Huang, Lu Yuan, Dong Chen, Ming Zeng, and Fang Wen. General facial representation learning in a visual-linguistic manner. In *Proceedings of the IEEE/CVF Conference on Computer Vision and Pattern Recognition*, pages 18697–18709, 2022. [6](#)
- [66] Zheng Zhu, Guan Huang, Jiankang Deng, Yun Ye, Junjie Huang, Xinze Chen, Jiagang Zhu, Tian Yang, Jiwen Lu, and Dalong Du. Webface260m: A benchmark unveiling the power of million-scale deep face recognition. In *CVPR*, pages 10492–10502, 2021. [6](#)
- [67] Zhuofan Zong, Dongzhi Jiang, Bingqi Ma, Guanglu Song, Hao Shao, Dazhong Shen, Yu Liu, and Hongsheng Li. Easyref: Omni-generalized group image reference for diffusion models via multimodal llm. *arXiv preprint arXiv:2412.09618*, 2024. [1](#)

HiFi-Portrait: Zero-shot Identity-preserved Portrait Generation with High-fidelity Multi-face Fusion

Supplementary Material

Appendix

In this appendix, we provide the following details:

- (1) A comprehensive statistics of our proposed dataset, presented in Sec. A.
- (2) A detailed description of the HiFi-Net architecture, featured in Sec. B.
- (3) Supplementary experiments, presented in Sec. C.
- (4) Further discussions, found in Sec. D.

A. Detailed Dataset Statistics

To train our proposed HiFi-Portrait, we construct a high-quality ID-based dataset. In this section, we count identities, the number of images, identity cluster size, face area, age and gender distribution, to highlight the diversity of our dataset.

Statistics for identities and images. As illustrated in Tab. 6, the dataset consists of three parts: VGGFace2-HQ [13], IMDB-Face [50], Web. Among them, VGGFace2-HQ is the high-resolution version of VGGFace2 [10]. Its images utilize face alignment; therefore, the face area is relatively large. To improve diversity, we download the source images of IMDB-Face and collect additional data from the Internet (abbreviated as "Web"). After extensive data cleansing and processing, our final dataset consists of 34k IDs and 960k images, averaging 28.2 images per ID, underscoring the diversity of identities.

Table 6. **Statistics of identities and images of our dataset.** It consists of three parts: VGGFace2-HD [13], IMDB-Face [50], Web (data we collected from the Internet).

Dataset	Identities	Images	Images/ID
VGGFace2-HD	8k	440k	55.0
IMDb-Face	21k	380k	18.1
Web	5k	140k	28.0
All	34k	960k	28.2

Identity cluster size. Fig. 11 presents the distribution of each ID cluster size. Ince the model training requires at least 1 target image and 4 reference images, ID clusters with fewer than five images are excluded.

Face area. Fig. 12 displays the distribution of face area proportions within the dataset, where the face area is defined

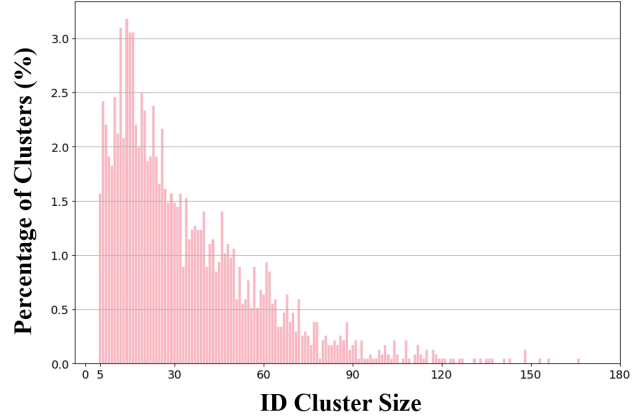


Figure 11. **Distribution of ID cluster size.**

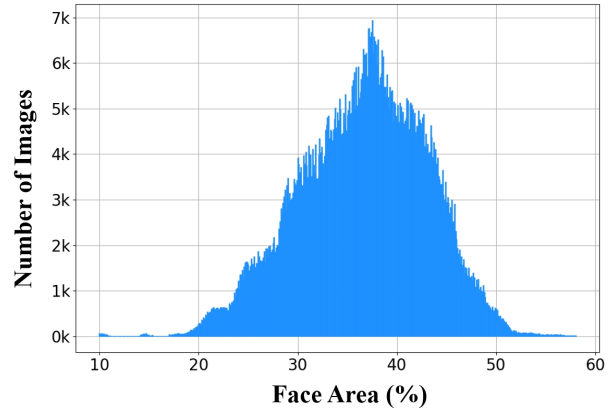


Figure 12. **Distribution of face area.**

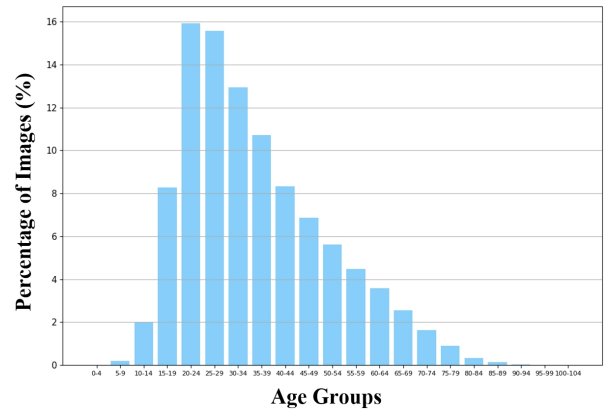


Figure 13. **Age distribution.**

Images	Prompts
	A young woman with blonde, wavy hair, wearing black-rimmed glasses and a patterned shirt, looking calmly at the camera with a blurred indoor background.
	A woman with styled blonde hair and red lipstick, wearing an elegant, strapless black gown with intricate lace-up detailing, poses in front of a dark background with white text.
	A woman with straight blonde hair and bangs, wearing red lipstick and a white blazer over a light-colored top, stands outdoors in a brightly lit urban setting with a blurred background.
	A woman with long, wavy blonde hair and bangs, wearing a yellow and black plaid corset-style dress with a matching choker, stands in front of a dark, patterned background with a bold design.
	A woman with wavy blonde hair and bangs, wearing red lipstick and a bright pink hoodie with printed lettering, poses outdoors with a blurred urban background.
	A woman with styled blonde hair swept to the side, wearing red lipstick and statement earrings, dressed in a black glittery outfit, looking off-camera against a warm-toned, striped background.

Figure 14. Some samples from the same ID group.

by the bounding box area predicted by RetinaFace [16]. The spacing on the x-axis is set at 0.1. We observe that images with small faces often feature blurry and distorted faces; therefore, we filter out images where the face area is less than 10%.

Age and gender distribution. Fig. 13 and 16 outline the distribution of age groups and genders, respectively. Here, age is estimated by Facelib [15]. For gender, both IMDb-Face and Web contain names, and we can retrieve gender by name. For images where gender could not be directly retrieved, we use Facelib to obtain their gender.

Dataset sample. In Fig. 14, we present several samples from the same ID group in the dataset.

B. HiFi-Net

The architecture of HiFi-Net is depicted in Fig. 15. We made two critical modifications compared to ControlNet [63]:

1. Face landmarks are used as input conditions to guide multi-face fusion, which enables more precise control over facial expressions and poses, thereby enhancing ID fidelity as illustrated in Fig. 6 and 9.

2. The cross-attention condition is multi-face features derived from the face refiner. Multi-face features capture more facial details than local and global features, as shown in

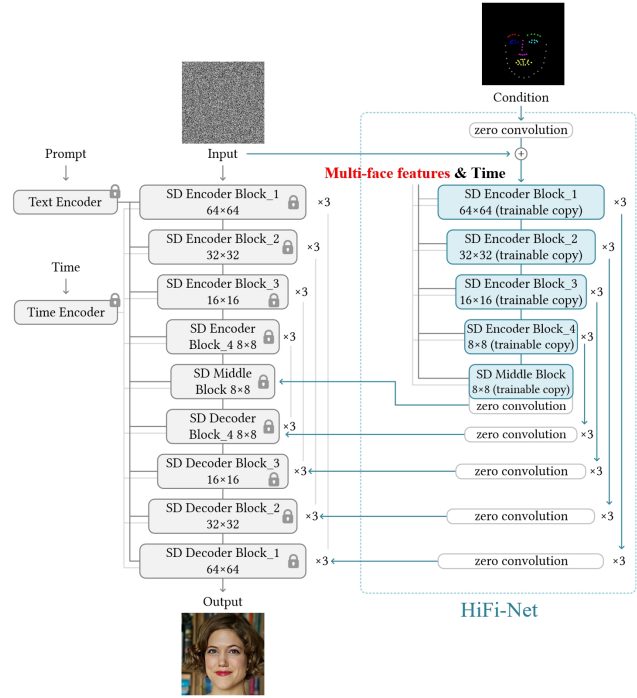


Figure 15. The architecture of HiFi-Net. The input condition is the face landmarks, and the input cross-attention condition is multi-face features. The landmarks guide the multi-face features to be effectively aligned and fused in HiFi-Net.

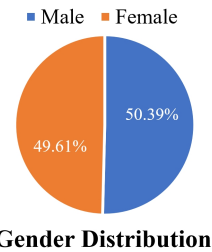


Figure 16. Gender distribution.

Fig. 8 and 9. In addition, compared with single-face features, multi-face features contain richer ID information, as shown in Fig. 10.

In summary, we employ HiFi-Net for effective multi-face fusion.

C. Supplementary experiments

C.1. Comparison with LoRA-based methods

Fig. 17 shows the qualitative comparison between HiFi-Portrait and LoRA-based methods [26, 34]. Our method demonstrates higher ID fidelity and precisely controls the face expression and pose.

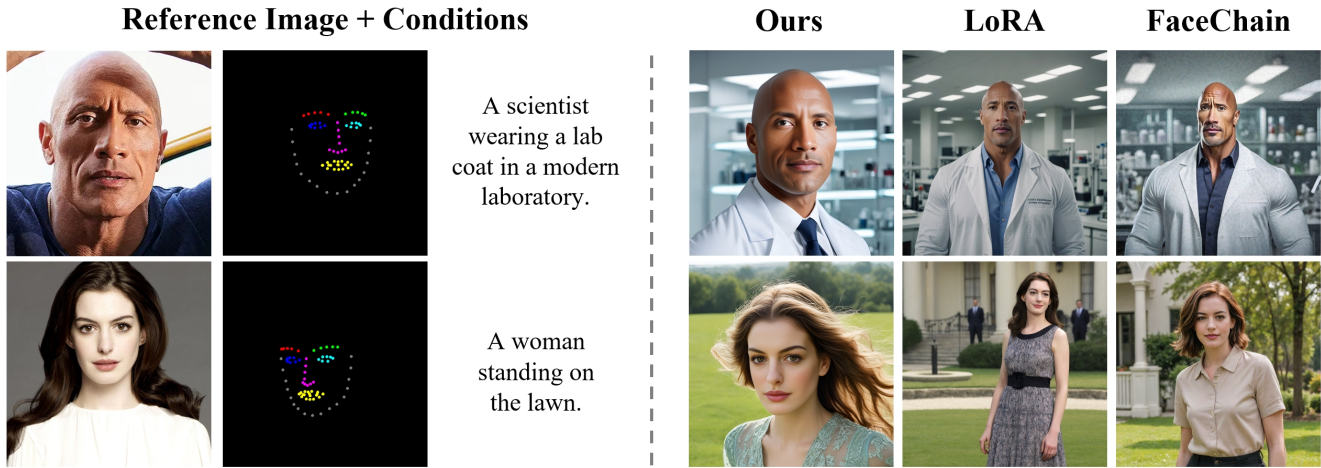


Figure 17. Comparison with LoRA-based methods. Our method exhibits higher ID fidelity.



Figure 18. HiFi-Portrait generates lighting that is more consistent with prompt. Zoom in the image for a better visual experience.

C.2. More challenging cases

Figs. 18–20 illustrates varying lighting, facial occlusion, and extreme expressions. Fig. 18 shows that HiFi-Portrait generates text-consistent lighting from multiple angles. Fig. 19 demonstrates more natural facial occlusions. Fig. 20 confirms that HiFi-Portrait effectively remains extreme expressions.

C.3. Input condition analysis

Fig. 21 reports results under different conditions. Col. 5 without text prompts or landmarks. Col. 6 uses text only.

Comparing Col. 7 (uses landmarks only) and Col. 8 (uses text and landmarks) demonstrates that using text prompt improves the alignment between target and generated expressions.

D. Further Discussion

D.1. Limitations and future works

The primary experiments in this study required approximately 1500 GPU hours on A800 GPUs. Therefore, we do not have enough computing power to explore some hyperparameter settings. Future research should focus on developing more



Figure 19. Our method generates more natural facial occlusions.

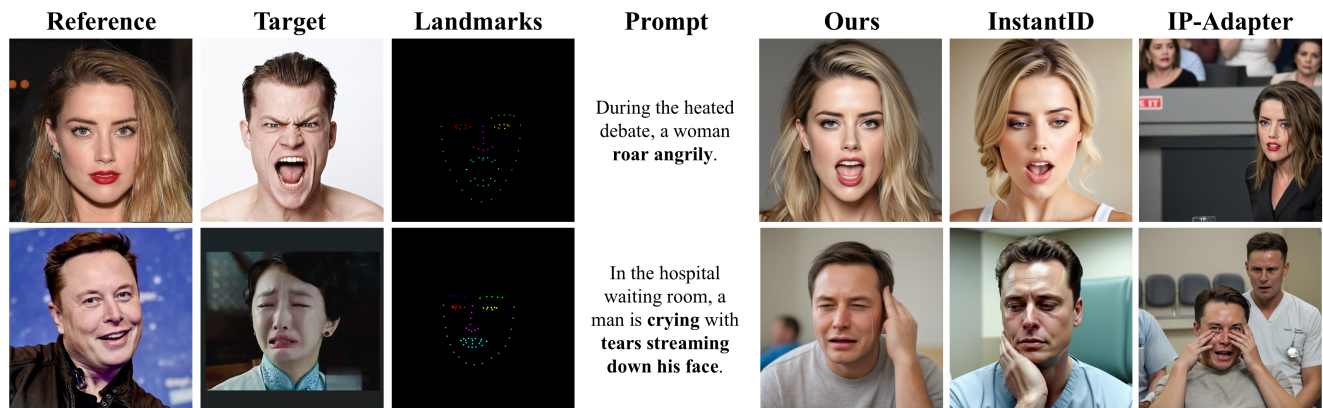


Figure 20. Our method effectively remains extreme expressions.



Figure 21. Using text prompt improves the alignment between the target and generated expressions.

straightforward and controlled models, rather than expending extensive efforts on hyperparameter tuning. Innovations such as a streamlined ControlNet-based method, ControlNext [37], or faster denoiser [33] could be beneficial. Additionally, experimenting with recent models like SD3 [17] or FLUX [2] may prove fruitful.

D.2. Broader impacts

This work contributes a high-fidelity framework for zero-shot ID-preserved generation to the open-source community, capable of customizing facial expressions and poses. Depending on the application context, this may have positive and negative impacts. On the one hand, our multi-face fusion strategy could advance the development of open-source ID-preservation models and use them in practical applications. On the other hand, the high fidelity of generated images could be misused for facial fraud.

D.3. Ethical considerations

To facilitate a more accurate understanding of human anatomy, SDXL utilizes a limited number of nude images for training. In our experiments, if clothing is not specified in the text prompts, there is a small probability that the generated portraits may be nude. Consequently, we recommend activating NSFW detection to minimize this issue. Additionally, the generative results have observed no other unethical or harmful behaviors. Finally, it is imperative to note that all data and models in this paper are intended strictly for research purposes and must not be used commercially.